

ISIM Detector Readout Reference Design: Cycle 1

L. Boyce¹, J. Caldwell¹, G. Cammarata¹, J. Gal-Edd¹, M.A. Greenhouse¹, C. Hartman¹, J. Isaacs², M. Jurotich¹, K. S. Long², C. McCreight³, B. Rauscher², K. Rehm¹, R. Martineau¹, R. McMurray, Jr.³, K. Shakoorzadeh, R. Stone¹, and J. Sutton¹

¹ NASA Goddard Space Flight Center

² Space Telescope Science Institute

³ NASA Ames Research Center

1 Introduction

The NGST Integrated Science Instrument Module (ISIM) is being developed through a structured approach to design evolution in which the overall system design is iterated through several scheduled cycles leading to adoption of a baseline design during late mission phase B (Geithner 1999). Each iteration updates a system reference design that is used to define cost and guide system trade studies. This document describes the ISIM Cycle 1 reference design for operation of NGST science instrument detectors including: operating modes, data conversion hardware, and data processing hardware. General detector requirements are discussed elsewhere (McCreight et al. 1999).

This reference design is intended for use by ISIM engineers, detector manufacturers, and detector test scientists. Our goal is to ensure that NGST detector technology development, flight data system development, and science instrument development proceed with a common set of assumptions and requirements prior to adoption of formal baseline interface requirements.

In Cycle 1, we have assumed that the complement of instruments recommended by the NGST Project Scientist in January 2000 (Mather et al. 2000) is the set of instruments that will be flown on NGST. This reference design must support a 64 Megapixel NIR camera, a 16 Megapixel NIR spectrograph, and a one Megapixel MIR camera/spectrograph. The NIR Camera will likely be split into 4 separate optical subcameras with (nearly) identical optical elements and filters feeding 16 Megapixel focal plane arrays (FPAs). The NGST project is supporting development of two NIR flight detector technologies, one based on InSb and a second based on HgCdTe. For the mid-IR, the Project is supporting development of Si:As flight detectors. This readout approach supports all these technologies.

In the following sections, we derive science requirements on detector operating modes, data conversion and processing from the Design Reference Mission (Smith 1999). We then develop the corresponding system engineering requirements. We discuss options for detector readout modes, and define an initial system design approach. Finally, we recommend a set of laboratory studies needed to support further evolution of this design.

2 Science Requirements

The science goals for NGST were originally suggested and explored in reports edited by Dressler (1996) and Stockman (1997). The Design Reference Mission for NGST is an attempt to incorporate these science goals into an observing program and as such, constitutes a quantifiable way to judge the success of all aspects of NGST, including the detector readout design. This observing program requires imaging over the spectral range 0.6-28 μ and spectroscopic observations over the range 1-28 μ m.

Table 1. Top 7 DRM Programs and Required Capabilities

DRM Program	Major Required Instrument Capabilities	Comments
1. Form. & Evolution of Galaxies-Imaging	Wide Field NIR Imaging (1/2) Wide Field visible & 10 μ m imaging (1/2)	112 days with 16 sq arc-min FOV
2. Form. & Evolution of Galaxies-Spectra	R = 100 & 1000 @ $\lambda=3.5 \mu$ m	98 days 20 days
3. Dark Matter	Wide Field NIR Imaging	192 days for 16 sq arc-min
4. Reionization Epoch	R=100 NIR spectroscopy	10 days
5. High z Supernovae	WF NIR Imaging & some spectroscopy	Uses data from DRMs 1 & 3
6. High z Obscured Galaxies	$\lambda= 8-28 \mu$ m wide field imaging R=100, 1000 spectroscopy	54 days/ FOV 4 sq arc-min 10 days
7. Physics of Protostars	$\lambda= 15-28 \mu$ m imaging R = 1000 spectroscopy, $\lambda = 6-28 \mu$ m	40 days 35 days

The seven highest priority programs, which are shown in Table 1, suggest that NGST will probably spend the majority of its observing time conducting large imaging and spectroscopic surveys with total integrations of 10^5 seconds or more per field. Although the maximum observable flux in each mode is not well established, some bright-end overlap with ground-based facilities is desired as a goal.

2.1 The Need for Low System Noise

As illustrated in Table 2 (taken from McCreight et al. 1999), the DRM requires observations that range from very low to relatively high backgrounds.

Table 2. NGST Expected Photon Backgrounds

Wavelength (μm)	Background Flux ¹		
	R=5 (photons $\text{s}^{-1}\text{pixel}^{-1}$)	R=100 (photons $\text{s}^{-1}\text{pixel}^{-1}$)	R=1000 (photons $\text{s}^{-1}\text{pixel}^{-1}$)
1	0.18	0.0053	5.3×10^{-4}
3	0.54	0.016	0.0016
5	3.8	0.11	0.011
10	320	9.5	0.95
20	2.9×10^4	870	87
30	2.7×10^5	8200	820

¹The background flux incident upon the detectors is expressed in units of photons $\text{s}^{-1}\text{pixel}^{-1}$. Since the telescope's point spread function is not yet known, we assume Nyquist sampling. Flux is independent of aperture because each pixel subtends solid angle $\Omega = (\lambda/2D)^2$ on the sky at each wavelength. Since actual instruments will have fixed pixel size, shorter wavelengths will be somewhat under sampled, while longer wavelengths will be correspondingly over sampled. We assume optical throughput of 50% for R=5 imaging and 30% for $R \geq 100$ spectroscopy.

Following McCreight et al. (1999), our approach will be to focus on general observations and effects, with minimal focus on specific observational programs.

In the near infrared (NIR), these programs place a premium on achieving zodiacal light limited wide field imaging and detector system noise limited multi-object spectroscopy. They push detector system performance by requiring low per sample noise simultaneously with long (≤ 1000 s) exposure times. In the NIR, the total noise requirement for a 1000 s exposure is $\mathbf{s}_{\text{total}} = 10 e^- \text{rms}$, with a goal of $\mathbf{s}_{\text{total}} = 3 e^- \text{rms}$ (McCreight et al. 1999). This total includes detector read noise, photon shot noise, noise in the dark current, and any other noise source in the system. In order to carry out the current DRM in 2.5 years, it would be necessary to reach the

noise goal. For short exposures, the current state of the art in flight detector noise performance is summarized in Table 3:

Table 3. Best noise performances of current flight detectors

	QE	Read Noise (e^-) Multiple	Dark Current (e^-/s)
SIRTF InSb	0.9	7	0.1
SIRTF Si:As	0.6	8	<1

In addition to read noise, it will also be important to control drifts and 1/f noise effects in the NGST detectors. In the case of NICMOS, these drifts caused an exposure-to-exposure variation in the DC level of 75 electrons, greatly complicating pipelined data reduction and in some cases reducing the achievable signal to noise of observations. For NGST, given that we wish to combine exposures taken over periods of days to weeks, it will be especially important to control such drifts. Based on the NICMOS experience, a reasonable minimum requirement would be that total drift should be comparable to pixel-to-pixel noise components in a 1000 s exposure, i.e. total drift required $\leq 10 e^-$ in 1000 s (where total drift includes drifts in both the FPA and readout electronics) with a more challenging goal of total drift $\leq 1 e^-$ in 1000 s. There is some promise that on-chip “reference pixels” will improve immunity to drifts in the pedestal sample. However, it is not yet certain that reference pixels that effectively combat drifts can be engineered into all candidate array technologies. Reference pixels are discussed in more detail in Section 3.3

2.2 Exposure and Readout Times

In the NIR, the maximum integration time will often be limited by cosmic rays, which corrupt a proportionally larger area of each image as this time increases. Rauscher et al. (2000) discuss the cosmic ray flux/exposure time trade space in detail. They find that acceptably deep, cosmic-ray-free images can be obtained by stacking reasonable numbers (11 or 12) of $t=1000$ s exposures. Although there is a tradeoff in non-uniform sensitivity, $t=1000$ s appears to be a reasonable upper limit on NGST integration times.

With regard to short NIR exposures, the DRM does not provide definitive guidelines. McCreight et al. (1999) require NIR readout times ≤ 12 s. This limit is not however a science-driven requirement. Rather, it arises from a combination of engineering considerations including the need to limit the number of independent analog outputs on an array and the data conversion speed in order to meet power budget constraints. From the point of view of overall efficiency, a faster rate, e.g. 5 sec, would be highly desirable.

Returning to the DRM, programs 6 and 7 place a premium on mid-infrared (MIR) performance. In this wavelength range, the requirements are somewhat different. In particular, the high photon fluxes shown in Table 2, in conjunction with the $1.0 \times 10^5 e^-$ MIR well depth requirement (McCreight et al. 1999), suggest that shorter exposure times ≈ 5 s may be required for 28 **mm** imaging, if the focal plane is Nyquist sampled near 10 **mm**. If the focal plane is Nyquist sampled at 5 **mm**, then this requirement can be relaxed to the same ≤ 12 s that applies to the NIR.

3 System Considerations

In addition to purely scientific requirements, there are a variety of system issues that must be taken into account, some of which are discussed below:

3.1 Terminology

In this document, we use the term Sensor Chip Array (SCA) to mean a single hybridized IR array. SCAs can be built up into a larger focal plane array (FPA) by integrating them to a packaged assembly that would be inserted into an instrument as a unit. NGST science requirements are met by SCA formats in the range of $1000^2 - 2000^2$ pixels. These SCA subunits must then be built up into 4k x 4k FPAs for the reference NIR camera and spectrograph designs. Note that, in this document, we follow the usual convention of referring to 1024 x 1024 and 2048 x 2048 devices as 1k x 1k and 2k x 2k arrays respectively.

There are a variety of ways to read IR arrays (see, e.g. McLean 1997). All involve resetting pixels to a reference level and then measuring the voltage on that pixel one or more times before the next reset. IR photons incident on the active area of the pixel liberate charge within the pixel discharging the voltage across the effective capacitance of the detector and the MOSFET. Ideally, the reset step would be exact, but in practice it is not. The difference in the voltage between the ideal reference level and the actual level is known as the offset or feed-through. The difference in the voltage between the offset and the level immediately after the reset is released is called the pedestal. The change in voltage due to IR photons on the active area is the “signal”.

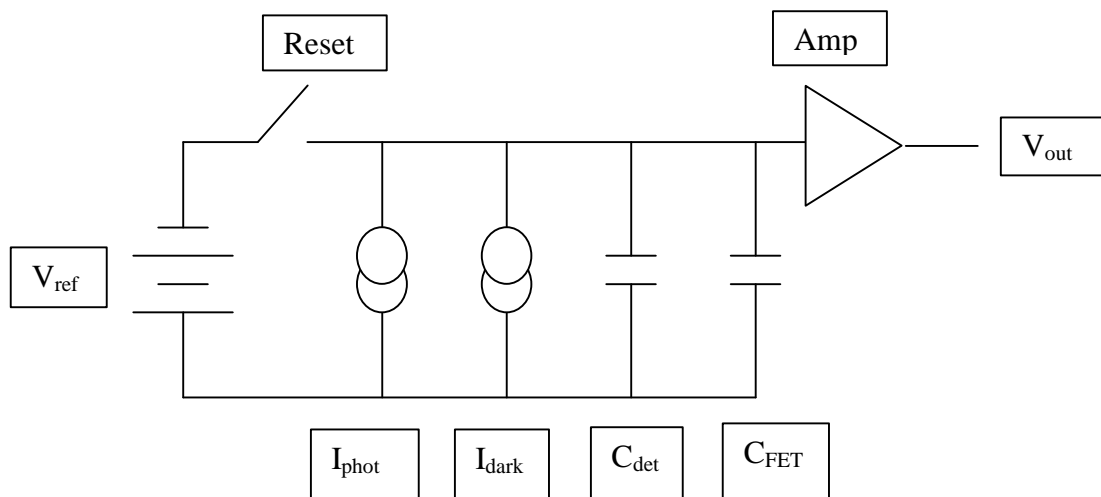


Figure 1: A simplified equivalent circuit for a single pixel in an IR array (omitting the complexity of multiplexer addressing.) The amplifier is typically a source-follower with gain less than 1.

Single sampling: In this scheme, the pixel is reset and then read after a time interval T_{int} .

Correlated Double sampling (CDS): Here the pixel is read once immediately after the reset and then read again after time interval T_{int} . (Note: According to McLean 1997, there actually are several ways in which CDS has been implemented, depending on whether one digitizes the reset level itself or not.)

Fowler sampling: In this approach, the entire array is reset, the entire array is read out non-destructively, and then after a time interval T_{int} the entire array is read out again. The effective signal is therefore given by

$$S_2 - S_1 = [(T_{ro} + T_{\text{int}}) \dot{N}_e + b + c] - [T_{ro} \dot{N}_e + b + c] = T_{\text{int}} \dot{N}_e$$

Note here that T_{int} refers to the interval between two reads for a specific pixel and \dot{N}_e is the rate at which electrons are produced due to the incident photon flux. The variables b and c are the amplifier bias and the unknown but correlated reset offset, or pedestal. (Note: See, e.g. Fowler & Gatley [1990] for an early description of Fowler sampling.)

Multiple Fowler sampling: In this approach, also known as Fowler(n), the entire array is reset, the entire array is read out n times non-destructively, and then after some time the entire array is read out n times again.

Here the sum of the initial reads is given by

$$S_1 = \sum_{m=1}^n (mT_{ro} \dot{N}_e + b)$$

and the sum of final reads is given by

$$S_2 = \sum_{m=1}^n ([mT_{ro} + T_{\text{int}}] \dot{N}_e + b)$$

and the difference

$$S_2 - S_1 = nT_{\text{int}} \dot{N}_e$$

is a measure of the signal. Here T_{int} is the time from the m^{th} read of a specific pixel in the first set of reads to the time of the m^{th} read of that pixel in the second set of reads. T_{int} defines the effective exposure time for a pixel.

Up the ramp sampling: In this approach, the entire array is reset, and then the entire array is readout continuously through the exposure. If the array is read out n times in this process, then the signal is given by the average of the slopes as measured in each of the reads:

$$\frac{1}{m-1} \sum_{m=1}^n S_m - S_{m-1} = T_{ro} \dot{N}_e$$

The power of up-the-ramp sampling is that it yields m-1 independent measurements of the flux.

3.2 Sampling

As indicated above, since the detector pixels can be read non-destructively, a rich array of readout options exist. The reason that there are so many ways to read out a IR array is due to the facts that (a) IR pixels can be read non-destructively and (b) pixels can be read in almost an arbitrary order (depending on multiplexer architecture), and (c) multiple reads do reduce system noise at low-light levels. It is not currently possible to specify the “right mode” for NGST since the final electrical architecture and exact characteristics of the detectors which will be flown are not yet known.

Consider a clocking scheme in which the given quadrant, say 1kx1k, is sequentially raster scanned from pixel (1,1) to pixel (1024,1024). The user has control of the speed at which this scan occurs. Consider a nominal pixel time of 10 μ s, which gives a scan time, T_{ro} , of 10.5sec, for a scan rate of about 0.1 Hz. This rate is probably within a small numerical factor of the speed we will use for a 1 Mpixel array.

Now assume a given observation time on any particular target, T_{tot} , of say 1000s. This time is the total frame time, including all clocking, resetting, and data acquisition. As noted above, this choice is probably within a small numerical factor of what will be used on NGST for NIR observations. The question then becomes, what sampling technique gives the best signal-to-noise ratio, for a particular set of noise sources?

A very general data acquisition that can be done with the above set up is to scan the array continuously $n=T/T_{ro}$ times during the frame time T, reading out the entire array each time. This approach also yields the simplest type of clocking to set up for an array. If n were large (which it is) small staggers in the scanning would not make much difference in the final noise numbers. The issue now becomes how often and exactly when to reset the array, assuming global reset which takes relatively very little time, and how to best use the data.

The simplest case is to reset only once at the beginning of T, scan n times at period T_{ro} and acquire all of the data. Now various analyses could be performed on this data set, including those needed to carry out up-the ramp sampling or (by discarding the middle n-2N samples) Fowler sampling. These approaches yield different effective noise, which integrates through the transfer function of the particular sampling algorithm. In addition to the above methods, one could conceive of readout approaches in which one scans a single row of the array multiple times before moving on to the next row. This option requires that rows can be individually reset, such as on the SBRC 744 multiplexer which is used for the four 256 x 256 arrays in the IRAC camera

of SIRTf. The disadvantage of this approach is that the time between samples on a given row is much shorter (a factor of 1024 for NGST) than for normal Fowler sampling. This time base does not allow good rejection of low frequency noise. In a certain sense, all of the N reads of a given pixel in this row by row method give nearly the same number. So they do not average the noise away, if the noise is due to low frequency drifts. The resulting reads are correlated on short time scales, and do not sample the slow 1/f changes. Since, in practice, low frequency noise is a serious issue in existing devices, we do not recommend pursuing this approach.

3.3 Noise Issues

As noted above, multiple non-destructive sampling of the signal during integration can provide significant improvement in the signal-to-noise (S/N) ratio of the acquired data compared to noise determined by conventional correlated double sampling (CDS). The two leading candidates for performing non-destructive reads are Fowler sampling (FS) and sampling-up-the-ramp (SUTR).

For Fowler sampling, one takes n samples of the pedestal, each sample separated by a scan time, T_{ro} , which might be about 10.5 sec for 1 Mpixel arrays read out at 10 microsec/pixel. One then takes n similarly spaced samples of the signal towards the end of the integration period which is typically about 1000 sec. In principle, if the time taken by the multiple readouts is small compared to the total time of the exposure (i.e. $T_{int} \sim T_{tot}$), and if the individual samples are statistically independent, then one obtains a SQRT (n) improvement in signal-to-noise (S/N) by Fowler sampling.

For uniform sampling up the ramp, one samples the ramp once per frame time interval starting from the pedestal and continuing for the entire integration period as frame after frame is taken. Using our example of a 10 microsec/pixel read rate, a 1kx1k array, and an integration time of 1000 sec, there would be roughly 95 such samples in an observation. In the SUTR technique, the average slope of these samples measures the signal and the noise can, at least in principle, be determined from the dispersion in the measured values of the slope from individual samples.

It is uncertain which components of the signal chain will dominate the 1/f noise, although there is some evidence that a portion due to FET offset drifts may be thermally driven. In the case of HgCdTe detectors, Marcia Rieke (pers. Com. 1999) has reported that the output FETs that Rockwell uses are extremely sensitive to temperature, showing variations in the bias $>500 e^-/C$. Additional low-frequency drifts may be due to bias voltage instabilities over these long time scales. In any event, 1/f noise is an inherent feature of oxide semiconductor devices, although the mechanism is not firmly tied down, and all candidate NGST detector technologies involve small MOSFETs.

The effectiveness of any sampling algorithm at improving signal to noise ratio is dependent on the exact character of the noise mechanism. For white spectral noise passing through the frequency transfer function of a sampling algorithm, noise can be reduced by root-N either by averaging N multiple reads of the pixel, or by reducing the bandwidth a factor of N. This reduction assumes the bandwidth is still large compared to the frequency at which a single pixel is read, as would still be the case if one row of 1024 pixels at a time were being read over and over for Fowler averaging, say at around 200Hz or 5ms row time. However, if the noise has a 1/f spectral characteristic, it does not help much to reduce bandwidth or to average on a short,

say row-by-row, time scale due to correlations in the signal values over these times. It is much more effective to spread out the readings over time and then perform an average with a long baseline.

The time baseline might be made even longer than the normal Fowler sampling by padding out the sample scans, roughly equivalent to using the data from every second or third scan in a continuous sequence. This sampling will reduce $1/f$ noise components out to smaller and smaller frequencies, but also reduces the average signal, as the effective integration time is the time from the first pedestal scan to the first signal scan. As long as the Fowler pedestal time is short compared to T there is little signal reduction. The worst case is when the first $T/2$ of the frame time is used for pedestal and the second $T/2$ for signal, since then the integration time is $T/2$ and the signal is only one half of the full signal integrated over the total time T . It would require a reduction in noise by a factor of two, usually meaning averaging four times as many samples, to make up for this signal reduction. This approach is not usually practical or even possible.

The frequency transfer function for a least squares fit up the ramp is very poor at rejecting low frequency noise, but again is fine for a white noise spectrum, or for a fixed distribution of read noise which appears time independent (same sigma over any time scale, so read noises are uncorrelated in time).

How do these sampling modes compare? The observations and conclusions depend on the dominant noise source, whether the sampling is read-noise dominated or background limited, and whether the noise is white noise or not (Garnett & Forrest 1993). NGST will observe in both regimes, both with the NIR detectors and with the MIR detectors.

For Read-noise Limited Performance one concludes that:

- a) If the read noise is dominated by white noise, both Fowler sampling (FS) and sampling-up-the-ramp (SUTR) are superior to correlated double sampling (CDS). Both FS and SUTR predict a $\text{SQRT}(n)$ improvement over CDS.
- b) Optimum Fowler sampling occurs if the pedestal and signal levels are each sampled for $1/3$ the total observing time, and the central $1/3$ of the integration time is not sampled. For our example, this would result in about 32 Fowler samples.
- c) In this case, SUTR would be predicted to be about 6 % better than FS. If this estimate reflects the performance improvement on real devices, then it would probably not be significant enough to justify the added computational complexity of the SUTR approach.

For Background Limited Performance (BLIP), where noise is dominated by photon shot noise, one concludes that:

- a) Unlike the read noise dominated case, successive signal measurements are correlated in their noise. Thus, it doesn't help to multiply sample, getting the same value each time, since there is no improvement by averaging these values.
- b) Correlated double sampling gives the best (S/N).
- c) SUTR is about 9% inferior to CDS.
- d) Fowler sampling S/N approaches that of CDS as the number of Fowler pairs approaches 1.

We conclude that both FS and SUTR are good sampling methods for the whole NGST performance range yielding much improved results in the read-noise dominated range and approaching CDS for photon-noise dominated operation. Of course this improvement is only realized if read noise is white. If the FETs have appreciable $1/f$ noise components, then the read noise will not see a $\text{SQRT}(n)$ improvement as the number of samples is increased.

The final paragraph of Garnett and Fowler makes an important point. They state that often, in an otherwise low background environment, the observing condition is such that there is a bright source and a dim source simultaneously imaged on the array. For this common case, Fowler sampling or sampling-up-the-ramp are superior sampling techniques. Both provide only slightly inferior (S/N) compared to CDS for the background limited source and enormous gain in (S/N) for the faint source buried in the read noise of the array.

3.4 Drift and Reference Pixels

As noted in section 2.1, drift was a problem with NICMOS on HST. This effect is a specific type of $1/f$ noise in which all of the pixels or at least all pixels on a given output line “drift” together. Laboratory testing shows that drift dominates $1/f$ noise in the IRAC detectors as well. The drift can be removed in a sort of DC-restoration or black level clamping, if it is known that some large part of the scene is black (an extended source which fills the entire array would preclude this procedure, and the common mode drift of the whole array would still appear in the signal as a noise source). Individual pixel drift or $1/f$ noise, from the integrating FET at the individual sense node, cannot be removed in this way. Standard Fowler sampling, in which the entire array is scanned before returning to a given sample, has been used successfully to average down this noise

Reference pixels may be used to mitigate the effects of drift, or very low frequency $1/f$ noise. The exact algorithm used depends on the type of reference pixels available. Let us assume a single extra pixel per row, all of which are good (no excess noise). Fowler sampling can then be performed exactly as before, with 1025 pixels per row rather than 1024. This is only a 0.1% overhead in terms of numbers to be downlinked. The reference pixel Fowler sum can then be used as follows to reduce noise.

On any given row, each pixel data sum consists of n signal reads minus n pedestal reads, for a total of n overlapped CDS samples (Fowler(n) sampling). The reference pixel at the end of the row also has a sum that is formed from n signal minus n pedestal values, each of which is within one row time (about 12 milliseconds) of the other pixels on that row. Taking the simple difference, in post-processing, of each pixel sum minus the one reference pixel sum on a row, is very much like a correlated triple sample (CTS). Rearranging the terms in the resulting difference, one can see that during each scan, a pixel value minus a reference pixel value is formed. The final sum is n such short-time differences of signal value minus n short-time differences of pedestal value.

The very short time difference of 6 milliseconds on average causes a transfer function whose first node extends out to 167 hertz. This extension causes a very low acceptance in the $1/f$ dominated region, in fact, lower by a factor of about 1×10^5 than the usual CDS or Fowler transfer function for 667 sec differences in optimal $1/3$ sampling of 1000 sec integration. The

signal value is the same as before, but drifts that occur on time scales longer than the 12 ms row scan time are rejected. This rejection greatly improves the signal to noise ratio. The above argument is only true for 1/f-dominated noise, since white noise would not be rejected by the short-time correlated sampling. Also, the noise must be common to both the pixel and the reference value, such as noise in biases, temperature, output FETs or amplifiers.

One big advantage to operating this way is that it does not take any additional hardware or software to implement, other than taking 1025 pixels of data per row instead of 1024. If there are more than one reference pixels per row, they can be averaged in post-processing to reduce noise further.

Having only a single reference pixel, or a small number, per entire 1kx1k array, does not give as good rejection of very low-frequency noise, but still allows post-processing subtraction of drifts on the time scale of full scans (12 seconds or so) and would still be a large improvement, of order 1×10^2 , in noise rejection over Fowler-only data. The average reference pixel Fowler sum is subtracted from each pixel sum in the entire array. The average time difference is now half a scan time or about 6 seconds. This approach is still an effective CTS algorithm since the CDS time differences are of order 667 seconds, a factor of 1×10^2 longer.

What could turn out to be a more important use of reference pixels would be in the SUTR algorithm. This method otherwise suffers from very poor 1/f noise rejection compared to CDS and Fowler. However, if during each row scan (or each full scan if only a few reference pixels are available) the pixel values are all differenced with the reference pixel, on a difference time scale of average 6 ms (or 6 s), the very low-frequency 1/f components (drift) are rejected by a factor of 1×10^5 (or 1×10^2). Once the 1/f component is not dominant, the least squares fit algorithm can be used to find the slope of the line, reducing the noise in the individual samples greatly. It is difficult to quantify the actual overall noise advantage here, but it is certain that common-mode 1/f will be rejected. This procedure could make the SUTR method a viable alternative to Fowler sampling. Again, if the 1/f noise is individual to a pixel, and not common to the pixel and reference, it will not be rejected and therefore this method does not give any improvement over standard SUTR. (Actually, using the extra samples in the calculation causes a noise increase by root-2.)

3.5 Computational Requirements

Fowler sampling can be easily implemented with a hardware coadder, and does not require a microprocessor. However, least squares fitting needed for SUTR does require on-board computational power, nominally something at the level of a DSP.

Memory requirements for Fowler sampling are one register, perhaps double precision if a large number of scans are coadded, per pixel. Memory requirements for least squares fitting up the ramp could be as large as keeping all of the ramp samples per pixel, for post computation, or keeping just four registers, two double precision and two quad precision, for sum x, sum y, sum x squared and sum x*y, per pixel if computation is performed on the fly.

3.6 Cosmic Ray Issues

When cosmic rays interact with a pixel of an IR array, that pixel and a small cluster of pixels surrounding it are corrupted. The average cosmic ray flux at L2 is high compared to that observed in low earth orbit outside the SAA. Indeed, it is expected to average between 5 and 10 $\text{cm}^{-2} \text{s}^{-1}$ (Isaacs et al. 1999). For a 27 (18) micron pixel IR array, a rate of 10 $\text{cm}^{-2} \text{s}^{-1}$, and a cluster size of 5, 36% (19%) of the pixels will suffer at least one cosmic ray hit in 1000 seconds. To zeroth order, this suggests that if one wants to build up an effective exposure time of 10,000 seconds out of multiple 1000 second frames, then one must plan on 3-4 additional exposures, implying a wall-clock time of as much as 14,000 s (see Rauscher, Isaacs and Long 2000 for a more complete discussion.) As a result, cosmic ray mitigation is a major consideration for readout strategies.

For Fowler sampling, data from any pixel hit by a cosmic ray is unrecoverable. In a Fowler scheme the only real way to reduce the amount of data that is impacted is to shorten the frame time. For example, if the frame time were 250 s, then one would still need to discard about 3-4 exposures, but in this case the wall-clock time would be ~11,000 s. In background limited cases, one can tolerate some reduction in the maximum frame time due to cosmic ray issues. However, in the case of narrow spectral bandwidth detector noise limited observations, the S/N grows roughly in proportion to t rather than \sqrt{t} , and reduced frame time would result in appreciable loss of sensitivity. Assuming adequate onboard computing power, ramp sampling offers opportunities for cosmic ray mitigation which do not suffer the disadvantages of Fowler sampling. The basic idea is to exclude outliers from the sample used to calculate the slope for a given pixel. A variety of algorithms to process the data have been considered (see e.g. Stockman et al. 1998). The basic reason that ramp sampling allows cosmic ray mitigation without requiring either additional exposures or loss of total S/N is that only the ~12 seconds of data between non-destructive reads is lost from the analysis process. Cosmic rays do not generally saturate the linear well of IR detectors and therefore if all the charge from a cosmic ray appears promptly then, in principle, cosmic ray mitigation could be effective. There are however at least two practical problems: (1) On-board cosmic ray mitigation requires substantial processing power (considerably greater than for ramp sampling without mitigation) and large amounts of memory (since all of the samples must be saved before processing can begin), (2) existing IR arrays, such as the NICMOS III detectors on HST, show both prompt and delayed release of charge as a result of a cosmic ray interaction. As a result, it is not currently clear that the signal in the sub-exposures following a cosmic ray interaction can in fact be used.

In summary, the issue of how best to handle cosmic rays is complex and the optimal exposure time will vary depending on the type of observation and on how much contamination of an individual frame can be allowed. At present, on-board cosmic ray mitigation is not within the baseline and studies are needed on real detectors to verify that it is possible at all.

3.7 A/D Accuracy Requirement

Under the assumption that NGST should be limited by the telescope background at, or by the detectors themselves when this is not possible (e.g., some spectroscopy), 18 bit A/Ds may well be required for both the NIR and MIR. There are three key inputs to this argument. First, there

are the detector goals and requirements as spelled out in McCreight et al. (1999). These are shown in Table 4.

Table 4. Detector Requirements

Total noise (e ⁻ rms)		Well depth (e ⁻)	
Requirement	Goal	Requirement	Goal
NIR	10	3	6 10 ⁴
MIR	20	3	1 10 ⁴

Second, the gain= g , measured in e⁻/ADU (equivalent to e⁻/DN), should be such that +/-1 bit errors do not compromise the total noise by more than 10%. Thirdly, using the resulting gain, it should be possible to digitize a saturated pixel.

Consider for example the case of the NIR detector goals. Assuming that A/D errors and detector noise are uncorrelated, these components add in quadrature and the required gain, allowing for 10% degradation of the total noise, is 1.37 e⁻/ADU. The full well value of 2.x10⁵ e⁻ corresponds to 1.46 x 10⁵ ADU, which cannot be represented with less than 2¹⁸ bits.

Applying this logic, 18 bits are needed to meet both the NIR and MIR detector goals. However, todays technology in the A/D arena for space applications at the NGST L2 enviroment, power, and data rates limits the choice to a 16 bit A/D converter. Fortunately, an attactive alternative exists to allow the use of a 16 bit A/D with the implementation of selectable gain on the A/D preamplifier. This approach is the recommended strategy for the Cycle 1 design.

3.8 Guide Mode

The NIR camera has a guide mode requirement of being able to use a single 1kx1k segment of a 4kx4k FPA to select and track a guide star under a 100 Hz control loop to generate fast steering mirror and S/C centering control commands. This ability must be incorporated into all of the 1kx1k segments of any of the 4kx4k FPAs, which cover the NIR field of view.

The guide mode requirement can, in principle, be accomplished using the same set of lines which operate a 1kx1k segment in normal use. Additional clock lines are not needed although the window, of nominal size 10 x 10 pixels, must be read out much faster than the segment itself. This readout is to be done by bursting to the window address, reading the window out at the normal pixel read rate, and then bursting to the next window read cycle. Using this technique, the entire window read cycle can be accomplished at nearly 1 kHz, well over the 100 Hz required for guiding. This approach to implementing the window requirement has been tested on actual

hardware and initial testing is encouraging. Further work remains to determine if there are any subtle effects, such as glow, which would interfere with science data acquisition in the remaining segments of the FPA. Using independent lines to address each 1kx1k segment, as envisioned, should allow the elimination of electrical pickup in adjacent segments being used for science data acquisition

3.9 Power Dissipation

For NGST, the power dissipated in the arrays are likely be the dominant source of heat within the cold portion of the ISIM and thus a critical parameter for determining how to keep the ISIM near its design requirement of 30 K. Both considerations imply that a major issue for readout schemes and detector designs will be to minimize array power dissipation. Power dissipation depends on how fast an array is read out. Using a minimum pixel read rate of 12 microseconds, a 1kx1k array having 1 output can be read out in about 12.6 seconds. If the array has 4 outputs, it can be read out in 3.15 seconds. Using an empirical rule of thumb that the average energy dissipated in array readout is 2 nJ/pixel/sample, one can calculate that the power dissipated in acquiring a frame of data from a 1kx1k array with 1 output is 0.17 mW, and is 0.67 mW for an array with 4 outputs read out 4 times faster. Unless there is a pressing need for very fast reads, the anticipated number of outputs per 1kx1k segment would be 1, and the resultant power dissipation is less than 0.2 mW. To be conservative, we have allotted a power dissipation of 1 mW perMpixel, even though there are indications that the 0.2 mW figure is itself conservative, and might actually become 50 to 100 microwatts. With the 1 mW/Mpixel allotment, the power dissipation for the 5(4kx4k) FPAs and the 1k x 1k MIR FPA would be 81 mW.

3.10 Fault Tolerance

A reasonable amount of fault tolerance is necessary to meet science objectives and still have a cost effective design. Ideally, one would limit single fault failures to the smallest independent sub-unit (1k x 1k array blocks). However, since power and mass are critical parameters, the current design assumes a 2k x 2k block failure requirement for the NIR FPAs. This design is shown in Section 5 of this report. For the MIR camera/spectrograph, which has only a single 1kx1k FPA, the adopted requirement is that no single failure shall affect more than a 512 x 512 block..

3.11 Summary

Given the early stage of the NGST detector development effort and our sparse knowledge of actual detector characteristics, the reference detector readout design should allow implementation of both multiple Fowler sampling and sampling-up-the-ramp. Sampling-up-the-ramp is more data intensive, but it might have advantages in accommodating data recovery from cosmic ray hits. It should provide a more uniform and stable chip temperature, unless addressing in a Fowler sampling continues to clock during the integration time without reading the data. One could think of taking the SUTR data stream, and using the appropriate 2/3 of the data stream to perform optimum Fowler sampling, or using the entire data stream for SUTR algorithms. At 10 microsec/pixel, the data rate for a single output 1kx1k array would be 1×10^5 samples/sec.

4 System Requirements/Assumptions for the Cycle 1 Readout Design

This section contains the actual requirements which the Cycle 1 Readout design is intended to address.

4.1 Detector Technology

The readout design shall support either InSb or HgCdTe for the NIR detector technologies; Si:As for the MIR detector technology.

For the purposes of the cycle 1 readout design, The linear well-depth for the NIR and MIR detector technologies is assumed $2 \times 10^5 e^-$. This represents the current goal values for the detector manufacturers. The current requirements are $6 \times 10^4 e^-$ and $1 \times 10^5 e^-$ for the NIR and MIR respectively.

4.2 Detector Complement

The Cycle 1 readout design will support a detector complement consisting of five each 4kx4k FPAs to support the NIR Camera and the NIR Spectrograph. Electrically, the NIR FPAs shall be addressable as 16 independent 1k x 1k arrays. In addition, the design will support one FPA for the Mid-IR Camera/Spectrograph, consisting of a single 1 k x 1k FPA. The MIR focal plane array shall be addressable as four 512 x 512 arrays. For the Cycle 1 design, we have assumed that the maximum allowable block of pixels which can be lost in a single point failure for the NIRCAM or the NIRSPEC cameras is 2k x 2k while for the MIR it is a single 512k x 512k subarray.

The number of pixels and their overall format is identical to the current design for NGST instrumentation. As discussed earlier, the requirement that the NIR focal planes be addressable as 1k x 1k derives from balancing fault tolerance and power and cost considerations against readout efficiency. The assumption that the MIR will be addressable in 512 x 512 subarrays is determined by expectations regarding Si:As detectors, the need for more rapid readout of these detectors at long wavelengths, and fault tolerance considerations.

Note: for the purpose of this design cycle, it is assumed that each SCA requires 9 biases, 5 clocks and 2 grounds.

4.3 Operational Modes

The readout design shall support science and diagnostic observing modes for the NIR and MIR detectors. In addition, for the NIR detector, the readout design will support a fast guiding mode.

4.3.1 Science Observations

Modes: For science observations, the detector readout design shall support both Fowler and linear up the ramp sampling for both NIR and MIR detectors. The number of Fowler samples shall be selectable (up to 32 at the beginning and end of the exposure in powers of 2). The readout design shall support continuous readout for the purpose of linear up the ramp sampling. If, as is assumed elsewhere, the detectors contain reference pixels, the design must support reading all of the reference pixels.

As discussed above, it is not possible to determine with confidence which of these two basic operational modes is optimal for NGST at this time, and therefore, the conservative approach is to support both..

Noise: The readout electronics shall not significantly degrade the performance of the NGST goal detectors of 3 electrons after multiple reads. For the purpose of this design the implied requirement is that the noise component contributed by the electronics shall be less than 1.5 electrons per read.

Readout rate: Detector readout time for a 1 Mega-Pixel NIR array will be ≤ 12 seconds, while for the MIR it will be 3 sec.

This choice is a compromise. Longer readout times than 12 (3) seconds will significantly reduce the observing efficiency unless the single read noise is very low. Shorter times are likely to compromise single read noise because there would be insufficient time for the A/D input to settle prior to digitization.

Dynamic Range: The readout design must allow for digitization over the full-well for each detector, although this requirement may be accomplished by gain control of the A/D pre-amplifier.

Including the possibility of a gain change is to allow use of 16 bit A/Ds. Otherwise it would be difficult to satisfy both the full well and noise requirement simultaneously.

Exposure Times: The readout will be optimized for exposure times between 200 and 1000 seconds; exposure times as short as 12 (3) seconds must be possible with reduced overall efficiency.

4.3.2 Fast Guide Mode

Modes: The readout design of the NIR cameras must accommodate a fast guiding mode in which an $n \times n$ pixel sub array centered on an arbitrary position is read from an individual 1k x 1k array. For a 10 x 10 sub array, the readout electronics must support a minimum rate of 100 Hz. The array to be used will be selectable, but no more than one such array will be read out at one time.

Noise: The readout electronics shall not significantly degrade the single read noise over that which is intrinsic to the detector

4.3.3 Diagnostic Mode

Mode: The readout design for both the NIR and MIR detectors shall incorporate a diagnostic mode in which all of the digitized data for an individual exposure is captured for a selectable 1 Mpixel section of any FPA.

4.4 Detector System Readout Requirements

Stability: The long-term gain instability between observations shall be less than 1%. This value assumes that reference pixels will be designed into the detector.

Fault Tolerance: No single fault shall affect more than a 2k x 2k area in the NIR and a 512 x 512 area in the MIR

The present baseline ADC requirement is 16 bits. The goal is to design for a selectable gain setting to be selected prior to an observation.

Cosmic Ray Processing: The readout design shall not include any special provisions for on board processing due to cosmic ray events.

Reference Pixels: The readout design shall include provision for the reference pixels, in on-board processing of Fowler or up-the ramp sampling, or demonstrate that for the particular algorithms adopted that it is not required. (Note for Fowler sampling, it is quite possible that the reference pixels can be processed in the same way that normal data pixels are processed and sent to the ground, while for ramp sampling it seems likely that the reference pixels must be subtracted from the data values prior to slope determination).

Efficiency: The efficiency of the readout (defined as the total useful data taking time) shall be greater than TBR (98%) under normal conditions.

Synchronicity: There is no science requirement to synchronize the readouts from the various detector blocks (1k x 1k or 512 x 512, although for electrical reasons they may be synchronized). However accurate knowledge (with TBD%) of exposure times for each pixel must be contained in the design..

Crosstalk: It shall be possible to operate any “channel” independently of any other channel without violating the requirements on noise.

FPA temperature stability: The FPA temperature shall be controlled to TBD mK.

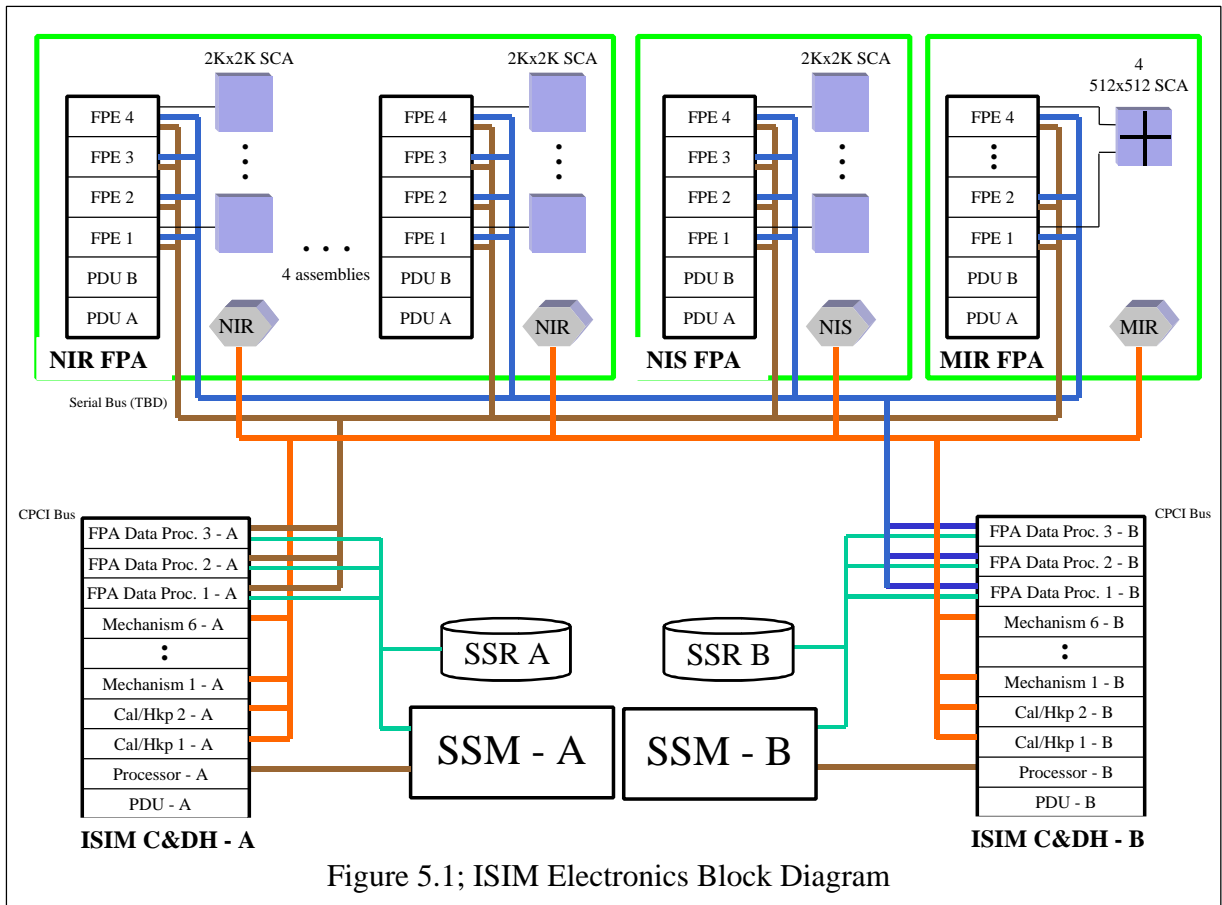
Temperature stability is a precondition for stable bias levels in NIR detectors and hence overall detector stability. The exact requirement is not currently known and will depend on the detector selected for NGST, but is expected to be of order a few mK. Larger drifts (degrees) result in changes in quantum efficiency.

Programmability: It must be possible to load and dump the FPA processor card.

Engineering data: Limit checking of the engineering data shall be performed for health and safety purposes.

5 Reference Design for ISIM Detector Readout Electronics

The detector readout electronics of ISIM consists of 24 fully independent functional blocks in order to meet the system fault tolerance requirements. Each functional block, referred to as a Focal Plane Electronics (FPE) herein, will contain all the necessary electronics to control and readout one cold SCA segment. A SCA segment is 2k x 2k for NIR and NIS, and 512 x 512 for MIR. Each FPE block is independently controlled and can be turned off in case of failure. A number of FPEs, i.e. 4, with some additional supporting electronics are grouped together in a box, referred to as FPA Electronics Box, which supports one camera assembly. See Figure 5.1 for the system block diagram.



5.1 Operational Modes

Science Observation Mode

In this mode, all the detectors are available for parallel observing at a stable temperature.

Sampling Modes

Pixels within a SCA segment will be sampled at 12 micro second intervals. For a 2k x 2k array, this will translate into a 12 second frame time.

Fowler Sampling Mode

The output of each detector in the array will be sampled number of times (N) at the beginning and n-times at the end of exposure period. The Fowler number, N, needs to be power of 2's. This will be implemented with a hardware co-adder. Memory requirements are one register per pixel plus N additional bits. A 2's compliment math will be used.

Sampling Up the Ramp Mode

The output of each detector in the array will be sampled number of times (M) at intervals optimized for an observation. The sampled data will be Least Squares fitted for each pixel. The number of samples, M, needs to be power of 2's. This will be implemented with a hardware math function. Memory requirements are one long register (at least 28 bits) per pixel and M additional words for the weighting value.

Guide Mode

This mode provides a searching and guiding capability using the fast steering mirror as the actuator and the FPA as the sensor to locate and track a target star during the observation. The output for guide mode is N-N pixels every TBD seconds with the field narrowing in predetermined increments to a 10 x 10-pixel area at 100 Hz rate. No additional hardware in the Detector Readout Electronics is associated with the guide mode. The same set of control lines and data readout out lines used for normal science data collection of pixel information is use for guide mode.

Diagnostic Mode

A Diagnostic Mode will be incorporated as necessary to verify proper operation of the data system. All data needed to reconstruct an expose will be collect for downlink.

5.2 FPE Readout Electronics Noise/Stability Budget

System FPR readout electronic noise and a stability budget are topics under study as part of the Cycle 2 tasks. The system noise of the detector readout is dependent upon the thermal temperature of the detectors, the readout scheme, the noise of the readout electronics, the noise induced on the detector cable themselves, and the Analog to Digital conversion process. A number of factor have to be considered to evaluated the actual system noise. Investigations into

the optimum detector harness material and shielding are underway. Plans are being made to measure and quantify the system readout noise at the time the flight like detectors are being characterized. The required total system noise is 10 electrons with a goal of three electrons.

5.3 Operation/Observation Efficiency

The goal of NGST will be to maximize observation efficiency. This is affected by a number of factors beyond the detector readout. The requirements for NGST operation and observation efficiency will be addressed in the next cycle of studies and requirements definition..

5.4 Hardware Functional Description

Each FPA has its own set of read and drive electronics, FPEs, to provide clock and bias signals to the arrays and do the required A/D conversions. All sets are identical. Other circuits control the calibrators and mechanisms and process instrument housekeeping data. A master sequencer controls internal instrument timing and multiplexing.

Functional and block redundancy is incorporated for all primary functions. No electrical single-point failure will cause a permanent loss of instrument functions. Redundant hardware is incorporated on A-side and B-side of electronics. Only one side is powered and operating at a time

Each FPE is made-up of the following functional blocks, as shown in Figure 5.2.

1. ASIC/FPGA

An ASIC/FPGA is incorporated within a FPE to interface with the FPA sequencer/ processor, generate all the FPA control timing signals, read the digitized signal from the A/D, perform the math computations, support DMA data transfer to the FPA processor, and generate additional required signals.

Computations:

Fowler sampling:

Data from each pixel will be processed according to the following algorithm:

(sum of second N reads) - (sum of first N reads)

Data will be further processed to obtain a 16-bit result (?) by retaining the highest-order data bits for the digitized signal.

Sampling up the ramp:

Data from each pixel will be processed according to the following algorithm:

$(\text{avg}(XY) - \text{avg}(X)\text{avg}(Y))/(\text{avg}(X^2) - (\text{avg}X)^2)$

X: time Y: Detector output

2. Memory

3. FPA Biases

The bias voltages depend upon the manufactures implementation. However, it is common to expect to have fixed bias as well as variable bias that are commandable in flight, independently in each channel

4. FPA Clocks
5. Pre-Amp
6. Digitizer
7. FPA Temperature Controller
8. Power Conditioning/Switching

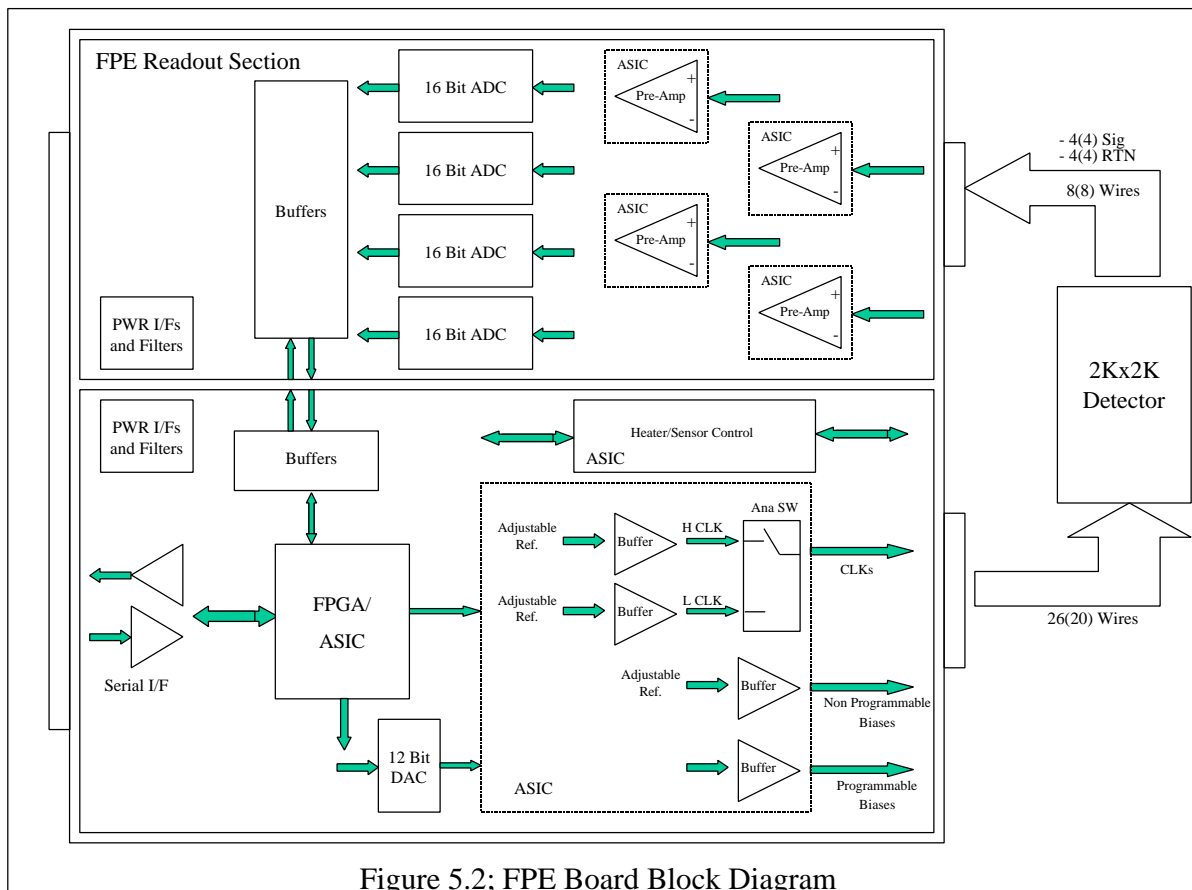


Figure 5.2; FPE Board Block Diagram

5.5 Software Functional Description

The following description is consistent with figures 5.1 and 5.2 above. The figures define a centralized single ISIM hardware architecture.

The FPA software described below will reside on the ISIM main processor card. The software shall interface directly to the FPA Data Processor cards across the cPCI bus within the ISIM box only.

Science Data Capture

The software will coordinate the collection and processing of the FPA data through 1 to 6 FPA Data Processing Cards within the ISIM C&DH Modules. The software science data capture process is as follows:

- 1) Receive software command to take an exposure (readout scheme)
- 2) The readout scheme is selected from the onboard stored sequences. A stored sequence is a set of detector processing instructions.
- 3) The set of detector processing instructions are loaded into the corresponding FPA Data Processing cards.
- 4) The detector processing commands are started via synchronized timed command to the FPA Data Processor card(s).
- 5) At the end of the data gathering (200-1000 seconds) the ISIM C&DH commands the FPA Data Processor Cards to transfer the data.

Guidance

The overall concept is that the Fine Guide Control function is resident onboard and has the control of this Guidance mode for a particular observation. The ground or sequence interface for guiding is done through the Fine Guide Control function. The Fine Guide Control function shall program the FPA Data Processor Card corresponding to the SCA segment selected for coarse track. When coarse track is reached the Fine Guide Control function shall reprogram the FPA Data Processor Control Card for fine lock which will be continuous until commanded otherwise. Once the start guide command is issued the data received from the FPA Data Processing Card shall be packaged and sent to the Fine Guide Control function.. The 10 x 10 at 100 Hz track mode is the highest data rate allowed. The guiding data received from the FPE Box may also be stored on the SSR or in local memory as selected. This allows diagnostic investigation of guiding problems after the fact.

Command and Data Handling

The ISIM CPU will execute a copy of the Common C&DH software. This software has the following capabilities:

Command Management

- All software components communications using command packets
- All commands are routed using the Command Manager
- Facilitates processor to processor/task to task communications

Telemetry Management Collects telemetry

- Filters and sends telemetry “packets” to the Telemetry Downlink component

Stored Commanding

- Provide Relative sequencing capability
- Sequences can be initiated by a software component
- Typically, sequences are provided to performing the following tasks: Failure corrective actions and/or Safing

Subsystem Telemetry Monitoring & Limit Checking

- A user defined set of telemetry points are monitored
- Each monitor has a set corresponding conditional expressions
- Many monitor points /w conditional expressions may be combined into a complex expression
- Then an expression evaluates to true a user defined action is taken (possibly initiate relative stored command sequence)
- Typically, conditional expressions are provided to performing the following tasks: Failure detection, Thermal monitoring, or Power monitoring

Memory Load and Dump - Manage flight memory

- Load high level Table (application variables or constants)
- Load flash memory (management only)

Dump high level application tables, direct RAM data, or Flash data

For more details on the complete NGST flight software system, refer to the "A Preliminary Descriptions of the Flight Software Functions [Balzano et al. 1999]", "NGST Flight Software Development and Test Environments [Rehm 1999]", and "Common C&DH Concepts [Cammarata 1999]."

5.6 Detector Readout Harness Design

The attachment of the detector system to the electronics with redundancy and independence requirements requires a large number of connections. Requirements of redundancy and independence produce a large number of wires in the system. The current architecture will be described here. A flat ribbon cable of twisted pair manganin with outer shield of vapor deposited copper or aluminum will be employed for each SCA of each FPA. This means that there would be 24 ribbons total for all of the SCA's (see Figure 5.3). The design will employ one or more thermal sink locations to shunt the heat load down the harness runs away from the FPA. At each of these sink locations, the harness wiring will also be interrupted at one or two locations per harness ribbon cable by “bridge” chips that will consist of a series of fibers of silicon or polyimid plated with copper or gold (see Figure 5.4). The “bridge” chips have heritage and are being used in other flight cryogenic systems now. Polyimid fibers may be preferred because experimentation in recent months has shown polyimid to be more robust and resilient to temperature changes and physical deformations. Each of the ribbon cable sections will have connectors on each end for ease of integration and assembly. The bridge chip mounting is

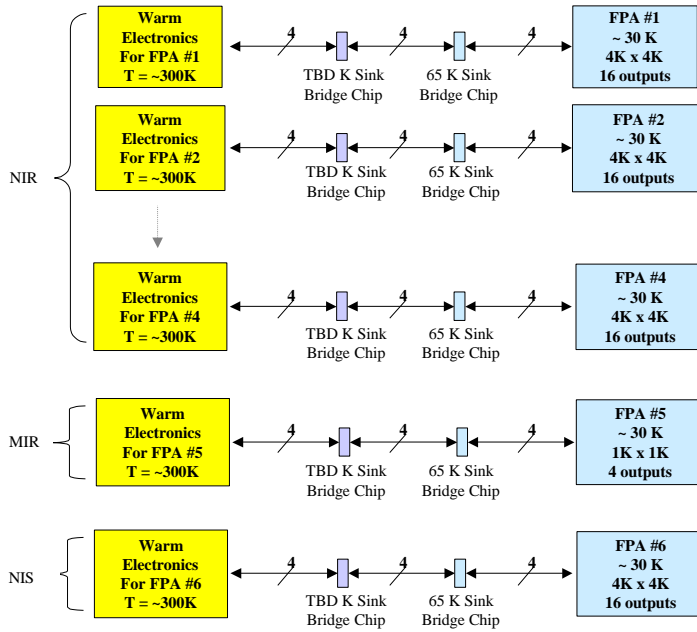


Figure 5.3 Detector Harness Configuration

4K x 4K Typical Harnessing

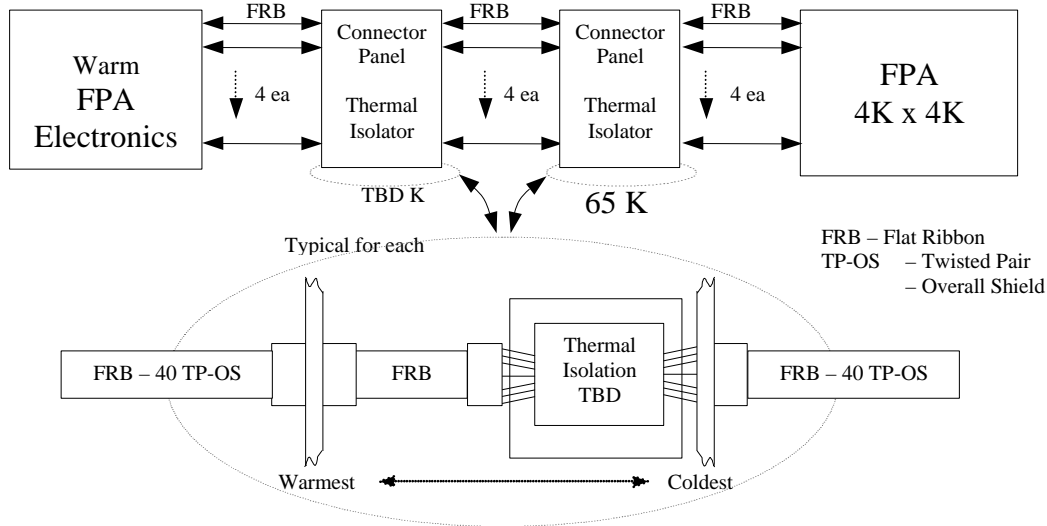


Figure 5.4 Bridge Chip Concept

currently envisioned to be housed in a G10 box and attached to a PC board with connectors on each end (see Figure 5.5). The connection concept of the bridge chip to the PC board in the box uses bump bonds so that in case of breakage, the chip can be replaced easily. Figure 5.5a shows an actual silicon bridge chip that uses bond wires rather than bump bonds which is a

viable concept also. The concept of using bridge chips is being investigated, and may or may not be used.

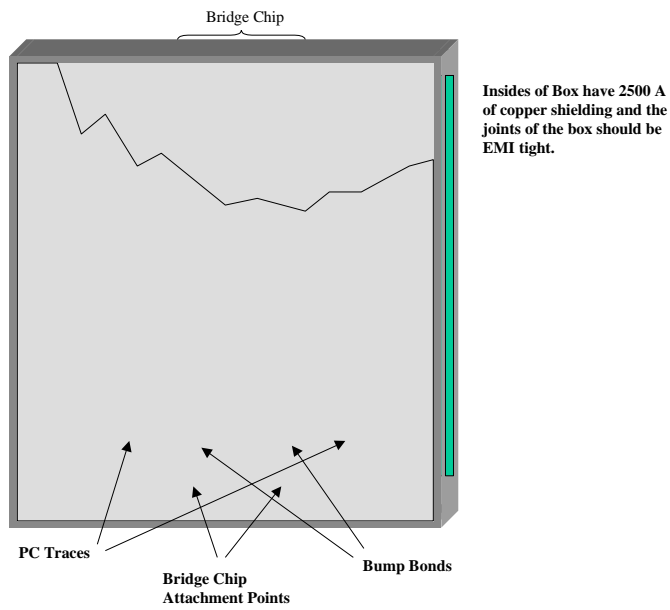
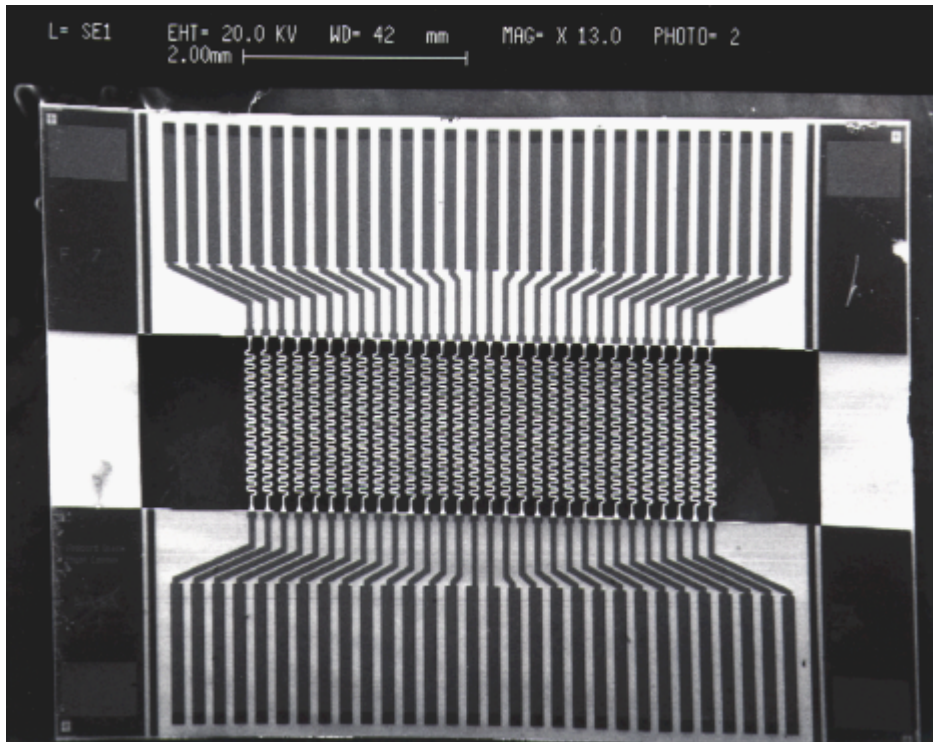


Figure 5.5 Thermal Isolator Conceptual Drawing

Bond Pads on thick frame

Laser cut Frame here

Bridges spanning air gap

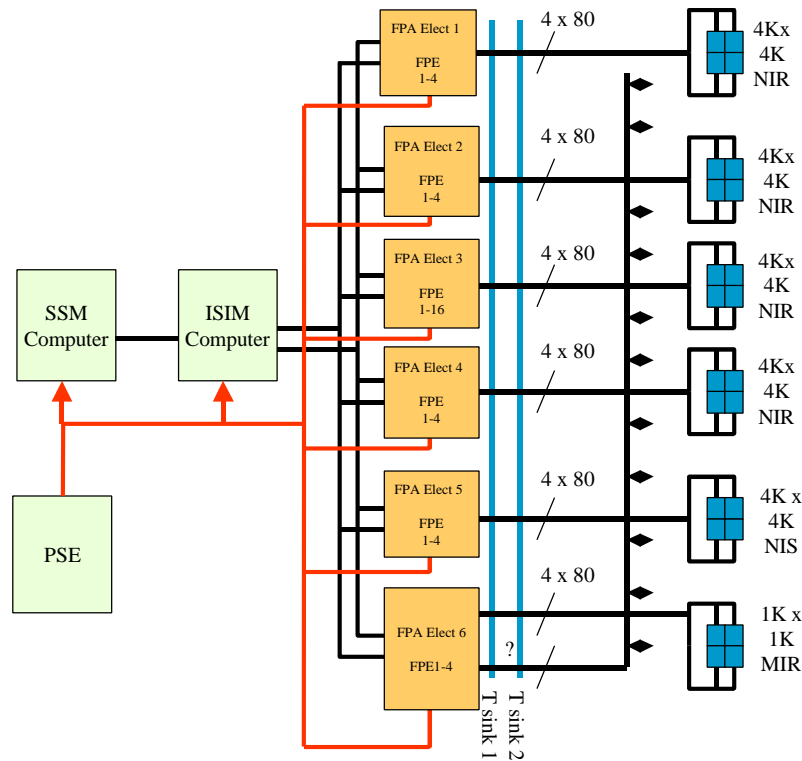


Pads for Thermal Jumpers

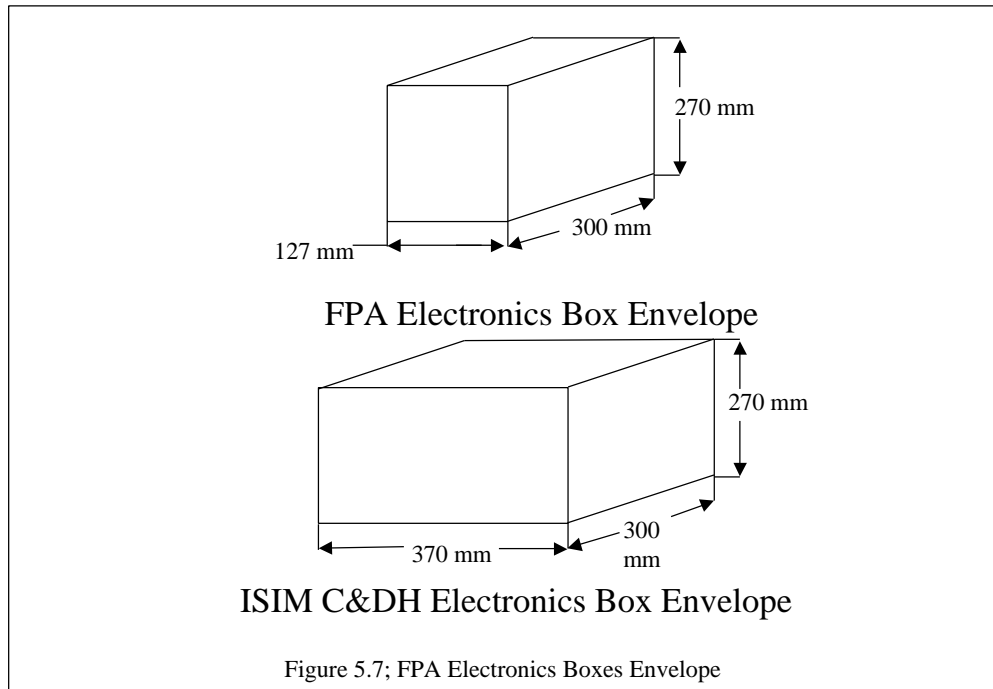
Figure 5.5a Actual Silicon Bridge Chip

The harness routing from the focal plane assembly will be in groups, one for each FPA Science data, one for each telescope mechanical control and monitor, and finally one for temperature monitoring of the telescopes. The length of the harness that runs from the FPA detector arrays to the FPA warm Electronics should be no longer than 3 to 4 meters. Longer runs will impact on the settling time of the signals and ultimately on the resolution and noise performance of the system. Each of the science data groups will terminate at its Focal Plane Electronics box located in the warm electronics bus area.

There are also other signals for temperature monitoring and control to the OTA and these must be considered in the thermal design of the system.



Detector Wiring Block Diagram
Figure 5.6



The FPA Electronics Boxes envelope are shown in Figure 5.7

FPA Electronics Box Mass (without margin)

The estimated FPA and C&DH Electronics Boxes has a mass of 88 (TBR). kg.

Harness Mass (without margin)

The estimated mass of the detector readout harness is 56 (TBR) kg.

FPA Electronics Box Power (without margin)

The estimated average power of the FPA and C&DH Electronics Boxes is 128 (TBR) Watts.

FPA Harness Heat Loss

Table 5.1 shows the thermal performance for heat loss in the FPA harness using manganin twisted pairs sizes #30 AWG to #40 AWG and not considering the bridge chips. The bridge chips should make the job easier and provide the capability of using lower impedance wire if the part can be realized and used for the temperatures ranges being considered.

Wire Size	Heat Loss	Pwr	R/Wire
#30 GA	338.2E-3	Watts	28.7E+0
#32 GA	222.3E-3	Watts	45.7E+0
#34 GA	147.6E-3	Watts	72.6E+0
#36 GA	99.0E-3	Watts	115.5E+0
#38 GA	67.1E-3	Watts	183.7E+0
#40 GA	46.1E-3	Watts	291.9E+0

Table 5.1

6 Recommended Empirical Studies in Support of the Readout Design

In many cases, the optimum choice of readout strategy, and to some extent the optimization of the overall ISIM readout design, depends upon very specific performance characteristics of the particular detector array technology. The report of the Detector Requirements Panel (NGST document 538) showed that while many aspects of the state-of-the-art of candidate focal planes are established (or can be projected with reasonable certainty), some important aspects have not yet been studied and understood. This is necessarily true, since NGST-optimized large-format prototype arrays are only now becoming available. NGST detector technology activities are yielding some early developmental arrays, with formats and sensitivity not yet up to NGST requirements and goals. As noted below, plans exist to support the testing of these devices. As time passes (as more capable prototype arrays are produced for NGST, and as a larger number of test groups become active in this work), one can expect that increasingly complete data sets will become available, to further guide ISIM readout system definition, and other elements of the system.

The following working list of items requiring additional experimental or analytical study has emerged from the deliberations of this team, and from the earlier Detector Requirements study. These data must be taken under anticipated NGST conditions. Specifically, these conditions include NIR array temperatures near 30 K (~6 – 8 K for the MIR range), low-background flux (extremely low, in the case of the highest-resolution spectroscopic measurements), and extended integration times of up to 1000 s.

1) Noise

1A) Studies of the spectral noise content of arrays, and experimental comparisons of sampling schemes (including Fowler, sample-up-the-ramp, & possibly others or variations). The parametric dependence of FET noise upon temperature, bias/current, and sampling factors (especially the time interval between samples, the total number of samples, and the specific averaging or weighting algorithms) must be determined.

1B) Studies of noise contributions from dark current: This will involve accurate measurements of the magnitude of dark current, and then the characterization of the noise contribution arising from these integrated charge samples. In particular, data are needed to ascertain if noise from dark current follows vn statistics.

1C) Additional noise factors: Careful, quantitative studies of non-white noise components including (but not necessarily limited to) bias drift ("pedestal effect"), shading, and 'bars & bands' are needed. In particular, it is important to determine how much of bias drift is electronic vs. thermal in origin.

1D) Studies of total noise: The overall noise level must be carefully determined, with specific interest in whether all contributing factors have been identified and whether these combine as theory predicts.

2) Additional resets or throwaway frames. Data are needed to determine the extent to which periodic resets will be needed, and how many throwaway data frames might be needed, under typical long-exposure conditions. These strategies are expected to restore stable operation to arrays, after a transient imposed by, for example, a slew to a location with a significantly different illumination level, a solar flare incident, a focal plane temperature excursion, a power transient, etc.

3) Reference pixels. Careful studies are needed to characterize the noise and stability of the reference inputs (e.g., on-chip capacitors mimicking detectors) being designed into current-generation candidate arrays. Techniques for best utilizing these inputs need to be developed and tested, with specific interest in how total noise [as in 1D) above] is affected.

4) Guide mode operation. Experimental data are needed to verify that guide-mode operation as described in Sec. 3 is achievable. One needs to verify that operation of a sub array at high frame rate does not contaminate data obtained from the adjacent low-rate science fields. Concerns include the possible presence of synchronous noise, glow effects (due to the higher current draw implied by higher frame rates), potential limitations on the ability to access an arbitrary field within the array, etc.

5) Driving exit cables. The focal plane outputs must be driven over many meters of cable to reach the first stage of amplification. It is important to test the ability of the output driver FETs on candidate FPAs to deliver signals over a simulated ISIM exit cable (with characteristics such as length, capacitance, and conductor geometry / shielding consistent with baseline ISIM designs). These data should indicate whether intermediate-temperature line-driver amplification must be included in the ISIM design. Key measurements will include noise, pickup, and transient response.

6) Power dissipation. Measurements are needed of power dissipation resulting from various candidates operating modes and sampling schemes. (Although this is primarily a driver for cryogenic and thermal control subsystem designs, the achieved dissipation levels couple to the data system design, in limiting number of samples, rate of samples, etc.)

7) Cosmic Rays. Data are needed of the sensitivity of the detector technologies to cosmic rays, including the amount of charge which bleeds into adjacent pixels, the time history of the release of charge due to cosmic rays, and the effectiveness of resets at removing cosmic rays.

General plans exist to conduct the measurements listed above, and as additional test groups are selected and support, the plans will become more specific. As summarized in Document 538, a small collection of PI and industry teams is presently assessing arrays coming from the NGST technology development contracts/grants, and the pace of this testing will be increasing.

Additional groups selected through the NGST Instrument Technology NRA (NRA-00-OSS-03) will soon supplement this team.

The presently supported test teams are evaluating noise (items 1A through 1D) and power dissipation. These teams are equipped to measure item 2), and when large-format arrays with on-board reference pixels are delivered (starting in CY 2000), item 3) can be studied. The Instrument Technology NRA will enable the testing of candidate NIR arrays in the guide mode, and data should be available in CY 2001. Plans for exit-cable testing have not been finalized, but it is very likely the appropriate capability will exist through the ongoing and supplemental NGST testing activities. As noted above, the detector development contracts are producing sample arrays, and this will continue at an increasing pace.

Given the wide range of potential array characterization parameters, it is essential that specific test plans and specifications, which specifically address these ISIM data system issues, be negotiated and instituted with the appropriate test teams.

References

Balzano, V., Cammarata, G., Doxsey, R., Gal-Edd, J., Greenhouse, M., Greville, E., Isaacs, J., Jurotich, M., Kalinowski, K., Kutina, R., Legg, J., Long, K., Rehm, .K, Welter, G., West, D., Whitley, R., 1999. A Preliminary Descriptions of the Flight Software Functions, Goddard Space Flight Center.

Cammarata, G., 1999. Common C&DH Concepts, Goddard Space Flight Center.

Dressler, A, ed. 1996, Explorattion and the Search for Origins: A Vision for Ultraviolet-Optical-Infrared Space Astronomy (AURA)

Fowler, A. M. & Gatley, I. 1990, ApJ, 353, L33

McCreight, C. et al. 1999, NGST Document 538, Recommendations of the NGST Detector Requirements Panel, 11 October 1999

Garnett and Forrest, 1993 SPIE, 1946, 395

Geithner P. 1999 NGST Doc 537, ISIM Phase 1 Plan

Isaacs J., Legg, J., & Thompkins, S. 1999, NGST Doc 584, The NGST Communications Study; Science, Data Volume and an Assessment of Communications Options

Mather, J., Jakobsen, P., Lilly, S., & Stockman P. 2000, NGST Doc. 549, NGST Science Instrument Recommendations

McLean I. S. 1997, Electronic Imaging in Astronomy: Detectors and Instrumentation (Wiley & Sons)

Rauscher, B.J., Isaacs, J., & Long, K. 2000, NGST Document 649, Cosmic Ray Management on NGST 1: The Effect of Cosmic Rays on Near Infrared Imaging Exposure Times

Rehm, K., 1999. NGST Flight Software Development and Test Environments, Goddard Space Flight Center

Stockman, H. S., ed. 1997, Next Generation Space Telescope, Visiting a Time When Galaxies Were Young (AURA)

Stockman, H. S. et al. 1998, NGST Doc. 160, Cosmic Ray Rejection and Imaging Processing Aboard the NGST

Smith, E., ed. 1999 NGST Document 472, Phase A Design Reference Mission